

Current-Voltage Analysis of a Tunnelling Emitter-Undoped Single Quantum Well Infrared Photodetector

K. K. M. N. Gurusinghe and K. Premaratne

Department of Physics, University of Peradeniya, Peradeniya, Sri Lanka.

T. G. Andersson

Applied Semiconductor Physics-MBE, Department of Physics and Engineering Physics,

Division of Microelectronics and Nanoscience,

Chalmers University of Technology and Göteborg University, Göteborg, Sweden.

and

S. V. Bandara

Center for Space Microelectronics Technology, Jet propulsion laboratory,

California Institute of Technology, Pasadena, California 91109, USA.

Abstract

The electrical behavior of a tunneling emitter-undoped single quantum well infrared photodetector (QWIP) structure was studied at 77 K. In order to understand the current generation and transport mechanisms, to estimate the quantum well electron density variation, and the barrier band bending under applied bias voltage, the current-voltage dependence was numerically analyzed using the known parameters of the structure. In this study resonance and non-resonance currents originated from the emitter contact, the field emission current from the quantum well, and also the thermionic emission current components were taken into account. The calculated and the experimentally measured currents were in good agreement. Also, the carrier density variation in the quantum well region and barrier band bending, as a function of bias voltage, were calculated.

I. INTRODUCTION

One of the most important application of semiconductor quantum wells (QWs) is in the detection of infrared (IR) radiation by utilizing intersubband photo-transitions between quantum states^{1,2}. Focal plane arrays of Quantum well infrared photodetectors (QWIP's) are of particular interest for generation of "IR images" in the 6-18 μm spectral band.

Operating these detectors at high temperatures is limited due to the dark current generated from the quantum wells and the contact layers. The optimization of the QWIP design requires the knowledge of the physical processes controlling the background dark current. Basic physical mechanisms behind the QWIP operation have been reviewed by Levine *et al.*³. In principle, the photon is detected by an excitation of an electron from a QW ground state to a higher state. These electrons are supplied by doping the quantum well^{3,4,5} or by tunneling into the well through a thin emitter contact layer^{6,7,8}.

Afterwards, excitation of the charge it is swept away from the QW to the collector contact due to an external electric field.

The infrared optical properties of the tunneling emitter-undoped single quantum well detectors (See Fig. 1) are particularly interesting because of the filling of the quantum well, and hence the optical response is strongly dependent on the bias voltage. The optical response of such a structure was first studied by Liu *et al.*^{6,7} using a fixed frequency CO₂ laser. Later Bandara *et al.*⁸ performed a series of experiments on a single

quantum well enclosed by asymmetric barriers, including measurements of the dark current, responsivity, and gain of such a detector.

In this work we have measured the dark current at temperature $T = 77$ K, and compared the results with numerical calculations in a similar tunneling emitter-undoped single quantum well structure. The structure, as shown Fig. 1(a), consists of an un-doped quantum well with thin emitter barrier and thick collector barrier, bounded by doped contact layers. The main idea of the asymmetric barriers was to tunnel electrons from the emitter to QW and suppress tunneling out of the QW. In our calculations, we take into account the electron conduction process through the structure, especially the resonance tunneling current from the emitter to the quantum well ground state energy level. The resonance tunneling current equation was derived using the transfer Hamiltonian description of resonance tunneling⁹, considering the emitter three dimensional electron gas and a two dimensional ground state energy level in the QW. Also the non-resonance current from the emitter, thermally excited field emission current from the quantum well, and the thermionic emission current components from the emitter and the quantum well were included in the numerical calculation.

This paper is organized in the following way. In Sec. 2, growth, processing of the used structure and the experimental techniques are described. In Sec. 3, the detailed theory and the current behavior are discussed. Next, the results and discussion are presented in Sec. 4. The asymmetry of the dark current in forward and reverse biased directions, the characteristics of the resonance current, voltage distribution among the barriers and electron density variation in the QW are presented. Our theoretical model provides a

good agreement between the calculated and measured current-voltage relation for several orders of magnitude in current.

II. DEVICE FABRICATION AND EXPERIMENTAL MEASUREMENT

The structure used in this work is shown schematically in Fig. 1a. It was grown by Molecular Beam Epitaxy (MBE) on a semi-insulating GaAs substrate with a 1 μm thick GaAs contact layer ($n=1.4\times 10^{18} \text{ cm}^{-3}$) on top, followed by a $L_c = 500 \text{ \AA}$ thick $\text{Al}_{0.27}\text{Ga}_{0.73}\text{As}$ collector barrier, a $L_w = 40 \text{ \AA}$ GaAs quantum well, and a $L_e = 150 \text{ \AA}$ thick $\text{Al}_{0.27}\text{Ga}_{0.73}\text{As}$ emitter barrier. Finally a 0.5 μm thick GaAs ($n=1.4\times 10^{18} \text{ cm}^{-3}$) contact layer was introduced. After growth of the structure, 200 μm diameter circular mesas were processed by standard photo-lithography wet chemical etching. Au-Ge ohmic contacts were evaporated onto the top and on the bottom contact layers.

The dark current through the structure for both forward and reverse directions was measured at 77 K in the bias voltages 0 to 500 mV with 10 mV increment steps. The forward bias direction refers to the emitter contact being negative (i.e. thin emitter barrier negative) and collector being ground (i.e. thick collector barrier ground) and vice versa (See Fig. 1(b)).

III. THEORY

In this part, the current components are described as a function of bias applied over the structure. The double barrier structure is shown in Fig. 1(b) with bias V_e across the emitter barrier and V_c across the wide collector barrier. The position E_r of the resonance energy level with respect to the conduction band minimum in the emitter contact layer is $E_r = E_1 - V_e$ ($E_r > 0$), where E_1 is the position of the ground state energy level in the quantum well. The sizes of the barrier potentials are given by the band edge offset ΔE_c . In the forward biased direction free electrons can tunnel to the QW region and be thermally emitted over the barrier. The rate of injection of electrons into the quantum well must be equal to the rate leaving it. These injected electrons can be treated as a resonance tunneling current $I_e^r(V_e, E_r)$ from the emitter contact layer to the ground state energy level E_1 in the quantum well and, the non-resonance tunneling current $I_{e_1}^{nr}(V_e)$ from the emitter in the energy range E_r to $(\Delta E_c - V_e)$. Due to the thick collector barrier there cannot be a resonance current from the quantum well energy state E_1 to the collector, only the thermally excited two dimensional field emission current $I_w^{fe}(V_c)$ from the quantum well. The current components across the structure are schematically shown in Fig. 1b. Injected electrons from the emitter to the quantum well are two contributions $I_e^r(V_e, E_r) + I_{e_1}^{nr}(V_e)$, which must balance the current between the quantum well and collector $I_w^{fe}(V_c)$. In principle there can be a transitional accumulation of two dimensional electrons in the well region. Note that the well is populated by the resonance current which mainly depends on the two dimensional quantum well Fermi energy E_F^{qw} (relative to the ground state energy E_1) and the three dimensional Fermi energy E_F^c of the contact layer, respectively.

In addition to the above current process there is a thermionic emission current above the emitter barrier, and a thermally assisted tunneling current $I_{e_2}^{nr}(V_e)$ from the triangular part of the emitter barrier (i.e. in the energy range $(\Delta E_c - V_e)$ to ΔE_c), which is not injected into the quantum well. Then the total current through the structure $I(V_e, V_c)$ is given by the Eq.s:

$$I(V_e, V_c) = I_e^r(V_e, E_r) + I_{e_2}^{nr}(V_e) + I_{e_1}^{nr}(V_e), \quad (1)$$

$$I_w^{fe}(V_c) = I_e^r(V_e, E_r) + I_{e_1}^{nr}(V_e). \quad (2)$$

In principle the resonance condition is fulfilled when the QW ground state is aligned with the Fermi level in the contact. However, we consider the system to be in resonance as long as the CB electrons in the emitter can tunnel to the QW ground state energy level E_1 . At off-resonance (i.e. the quantum well ground state energy level has dropped below the emitter conduction band edge; $E_r < 0$) there will be no accumulation of carriers in the quantum well and the total current is given by

$$I(V_e, V_c) = I_e^{nr}(V_e) + I_w^{fe}(V_c). \quad (3)$$

Here, $I_e^{nr}(V_e)$ is the current in the energy range zero to ΔE_c (i.e. from the conduction band minimum). The field emission current from the empty-quantum well is due to the thermal generation of carriers.

The externally applied bias voltage through the structure V_b is given by the Eq.

$V_b = V_e + V_c + V_w$, where V_e , V_c , and V_w are the voltage distributions among the emitter barrier, collector barrier, and quantum well, respectively. The relation between these voltages are given by^{3,4,8}

$$[V_e C_e - V_c C_c] = 2V_w C_w = -enAL_w. \quad (4)$$

Here the capacitance of the thin emitter, thick collector and quantum well are given by $C_e = \epsilon_2 A/L_e$, $C_c = \epsilon_2 A/L_c$ and $C_w = \epsilon_1 A/L_w$, respectively, and ϵ_1 and ϵ_2 are the permittivities of the well and the barrier regions. The symbols L_e and L_c are the thicknesses of the emitter and collector barriers, and L_w is the thickness of the QW. The average three dimensional electron density n in the well can be given by

$$n = \left(\frac{m_l k_B T}{\pi \hbar^2 L_w} \right) \ln \left(1 + \exp \left(\frac{E_F^{qw}}{k_B T} \right) \right). \quad (5)$$

The symbols have their usual meaning. In this study the main interest is the resonance current which is calculated by the "Transfer Hamiltonian formalism" considering tunneling of electrons from the three dimensional electron gas in the emitter to the two

dimensional electron gas in the quantum well. The resonance current can be shown to be⁹

$$I_e^r(V_e, E_r) = \frac{2eXm_1^2 Ak_B T}{\pi \hbar^5} \frac{|M_{e \rightarrow w}|^2}{k_r} \cdot \ln \left[\frac{1 + \exp\left(\frac{E_F^e - E_r}{k_B T}\right)}{1 + \exp\left(\frac{E_F^{qw}}{k_B T}\right)} \right], \quad (6)$$

where $|M_{e \rightarrow w}|^2$ is the matrix element for the transition from emitter to quantum well.

The analytic expression is obtained by matching wave functions that are solutions of the Schrödinger equations for emitter and QW regions and given by

$$|M_{e \rightarrow w}|^2 = \frac{\hbar^8}{Xm_1^2} \frac{k_r^4 K_r^3 \exp(-2K_r L_e)}{[E_r(m_2 - m_1) + m_1 \bar{E}_b]^2 \left[L_w K_r + \frac{2m_2 \bar{E}_b}{E_r(m_2 - m_1) + m_1 \bar{E}_b} \right]}. \quad (7)$$

Here X is the length of the contact layer which will cancel out, A is the device area, m_1 , and m_2 are the effective electron masses in the GaAs and $\text{Al}_x\text{Ga}_{1-x}\text{As}$ layers,

respectively. The symbol \bar{E}_b is the effective mean barrier height for the emitter barrier

$\bar{E}_b = (\Delta E_c - V_e)/2$, where ΔE_c is the conduction band discontinuity given by the

aluminum alloy composition. The symbols k_r and K_r are given by

$$k_r = \sqrt{\frac{2m_1 E_r}{\hbar^2}}, \quad K_r = \sqrt{\frac{2m_2 (\bar{E}_b - E_r)}{\hbar^2}}. \quad (8)$$

The non-resonance tunneling current from the emitter and the two-dimensional field emission current from the well are given by the Eq.s (9) and (10).^{3,4,8}

$$I_e^{nr}(V_e) = \left(\frac{em_1 k_B T A}{2\pi^2 \hbar^3} \right) \int_0^\infty T^e(E, V_e) \cdot \ln \left[1 + \exp \left(\frac{E_F^e - E}{k_B T} \right) \right] dE \quad (9)$$

$$I_w^{fe}(V_C) = \left(\frac{em_1 A}{\pi \hbar^2 L} \right) v(V_C) \int_{E_1}^\infty T^c(E, V_C) \cdot \left[1 + \exp \left(\frac{E - E_1 - E_F^{qw}}{k_B T} \right) \right]^{-1} dE \quad (10)$$

Here T is the temperature and $T^e(E, V_e)$ and $T^c(E, V_C)$ are the non-resonance tunneling coefficients given by the WKB approximation for the emitter and collector barriers respectively. In order to calculate the thermionic emission current, the tunneling coefficients were assumed to be unity above the barriers. In Eq. 10 the thickness L is $L = L_w + L_c$. The collector velocity $v(V_C)$ is given by^{4,8,10}

$$v(V_C) = \frac{\mu F_C}{\sqrt{1 + \left(\frac{\mu F_C}{v_s} \right)^2}}, \quad (11)$$

where $F_C = V_C/L_C$ is the collector electric field, μ is the mobility, and v_s is the electron saturation velocity.

IV. RESULTS AND DISCUSSION

The dark current across the structure was measured from 10 to 500 mV at liquid nitrogen temperature for both forward and reverse directions. In our structure the forward biased direction is with positive bias on the substrate. The current-voltage behavior at 77 K is shown in Fig. 2. The reverse current is one order of magnitude larger than the forward current, and the overall shape of the curves are similar except for a broad peak in the forward current due to the resonance contribution. Here we focus on the process generating the forward current which is of direct interest as it is a limitation in the QWIP performance. In the forward direction, the current, shown in Fig. 2, increased steadily in the interval 10 to 320 mV with a pronounced kink (denoted by the arrow) at around 150 mV. After passing through a broad resonance peak at around 350 mV, the current again started to increase steadily from 410 mV upwards.

The dependence of the current in the bias range 10 to 410 mV is described Eq. (1) under the condition given by Eq. (2). For bias voltages larger than 410 mV where E_1 has dropped below the conduction band minimum, the behavior can be explained by Eq (3). Figure 3 shows the comparison of theoretical and experimental forward IV characteristics. In this work, we have included the resonance tunneling, non-resonance tunneling and thermionic emission current contributions as described in the Eq. (1) to (11) and the dark current was calculated for the structure at $T=77$ K. The result is shown by the circular symbols in Fig. 3. In the numerical calculation for $E_r > 0$, the quantum well Fermi energy E_F^{qw} was calculated under the condition given by Eq (2) and fitting the mobility $\mu=2000$ cm²/Vs and $v_s=5 \times 10^6$ cm/s in Eq (11). After dropping of E_1 below the conduction band (i.e. $E_r < 0$) the total current was calculated according to the Eq

(3). The calculated points in Fig. 3 describe the general increase of the dark current and apparent the broad peak in the 300 – 360 mV bias voltage range resulting from resonant tunneling. Figure 4 shows the calculated resonant tunneling contribution to the total dark current as bias voltage varies across the device and it maximizes around 350 mV bias voltage.

In order to understand the appearance of the reproducible kink at 150 mV the resonance current variation was carefully investigated with bias voltage. In the calculated resonance current, which is shown in Fig. 4, has a minimum at around 135 mV.

Negative current below 200 mV indicates a change in the direction of the resonance current (i.e. from well to emitter contact). This minimum resonant current (or maximum reverse-resonance current) around 135 mV could be the reason for observing a kink in the experimental forward current. However, our forward current calculation did not indicate any kink at 135 mV bias or elsewhere. Furthermore, the difference between the voltages corresponding to the experimental kink and the theoretical resonance current minimum is 15 mV. These differences could be due to the possible uncertainty in the parameter values of the structure, such as aluminum alloy composition, thicknesses of the $\text{Al}_x\text{Ga}_{1-x}\text{As}$ layers and GaAs layer and doping density in the contact layers used in the calculation.

Also results of this calculations provide bias voltage distribution across the barriers and the quantum well and the variation of carrier density in the quantum well. The theoretical and experimental results both gave the resonance peak at 350 mV bias. The calculated voltage distribution across the structure is shown in Fig. 5. Most of the

applied bias voltage drops across the collector barrier because of the efficient tunneling through the relatively thin emitter barrier. As shown in Fig. 5, the rapid increase in the emitter voltage (V_e) around $V_b > 350$ meV is a result of the dramatic drop in the resonant tunneling contribution to the total current. See Fig. 4. Simple band structure calculations indicate that the GaAs QW of thickness 40 Å with $\text{Al}_{0.27}\text{Ga}_{0.73}\text{As}$ barriers has only one bound quantum energy state with energy ~ 90 meV. The Fermi energy of the contact layer was calculated to be 68 meV using the free electron model. For a total voltage drop of 350 mV across the structure the emitter barrier voltage was 47 mV. These results indicate that $E_r=43.6$ meV corresponds to the maximum resonance current. Therefore, our study indicates that the maximum resonance current does not necessarily occur at the point where the ground state energy of the QW aligns with the emitter conduction band minimum. Similar behavior in resonant tunneling current were predicted by Schulman¹¹ and explained by considering different *in-plane* effective mass in the emitter and well. Fig. 6 shows the calculated electron density variation in the QW under bias. The drop in electron density at higher bias voltages is due to decrease in the resonant tunneling current as indicated in the fig. 4. Unlike in previous calculations⁸, the non-abruptness in the decreasing electron density may have resulted from non-zero operating temperature and inclusion of finite size of the barriers in the resonant tunneling formula (Eq. 7). The electron density is observed to be maximum at 320 mV. Therefore, the photocurrent of the structure is expected to show similar behavior with a peak at 320 mV.

V. CONCLUSION

Well agreement between theory and experiment indicates that the carrier transport process through such quantum well structures is due to the combined effects of resonance tunneling, non-resonance tunneling, and thermionic emission. This theoretical model predicts the variation of electron density in the quantum well, and barrier band bending with the applied bias voltage, that are valuable in understanding and optimizing undoped tunneling QWIP device structures.

VI. ACKNOWLEDGEMENT

A part of the research described here was performed by the Center for Space Microelectronics Technology, Jet Propulsion Laboratory, California Institute of Technology, and was sponsored by the National Aeronautics and Space Administration, breakthrough sensor & instrument component technology thrust area of the cross enterprise technology development program.

REFERENCES

1. B. F. Levine, K. K. Choi, C. G. Bethea, J. Walker, and R. J. Malik, Appl. Phys. Lett. **50**, 1092 (1987).
2. L. C. West and S. J. Eglash, Appl. Phys. Lett. **46**, 1156 (1985).
3. E. Rosencher, F. Luc, Ph. Bois, and S. Delaitre, Appl. Phys. Lett. **61**, 468 (1992).
4. K. M. S. V. Bandara, B. F. Levine, R. E. Leibenguth, and M. T. Asom, J. Appl. Phys. **74**(3), 1826 (1993).
5. D. D. Coon, R. P. G. Karunasiri, and H. C. Liu, J. Appl. Phys. **60**, 2636 (1986).
6. H. C. Liu, G. C. Aers, M Buchanan, Z. R. Wasilewski, and D. Landheer, J. Appl. Phys. **70**, 935 (1991).
7. H. C. Liu, G. C. Aers, M Buchanan, and Z. R. Wasilewski, Semicond. Sci. Technol. **6**, C124 (1991).
8. K. M. S. V. Bandara, B. F. Levine, and M. T. Asom, J. Appl. Phys. **74**(1), 346 (1993).
9. M. C. Payne, J. Phys. C **19**, 1145 (1986).
10. B. F. Levine, C. G. Bethea, G. Hasnain, V. O. Shen, E. Pelve, R. R. Abbott, and S. J. Hgcih, Appl. Phys. Lett. **56**, 851 (1990).
11. J. N. Schulman, Appl. Phys. Lett. **72**, 2829 (1998).

FIGURE CAPTIONS

Fig 1. : Schematic conduction-band diagram of the undoped single-well QWIP. (a) under zero bias. (b) under a forward bias. The ground state electron energy level is indicated as E_1 . Also shown are emitter and collector Fermi energy levels, voltage drop across the barriers, and current components.

Fig 2: Experimental dark current at $T = 77\text{K}$ vs forward bias (positive) and reverse bias voltage. The arrow indicates a reproducible kink around 150 mV forward bias voltage. which may be resulted reverse-resonance current.

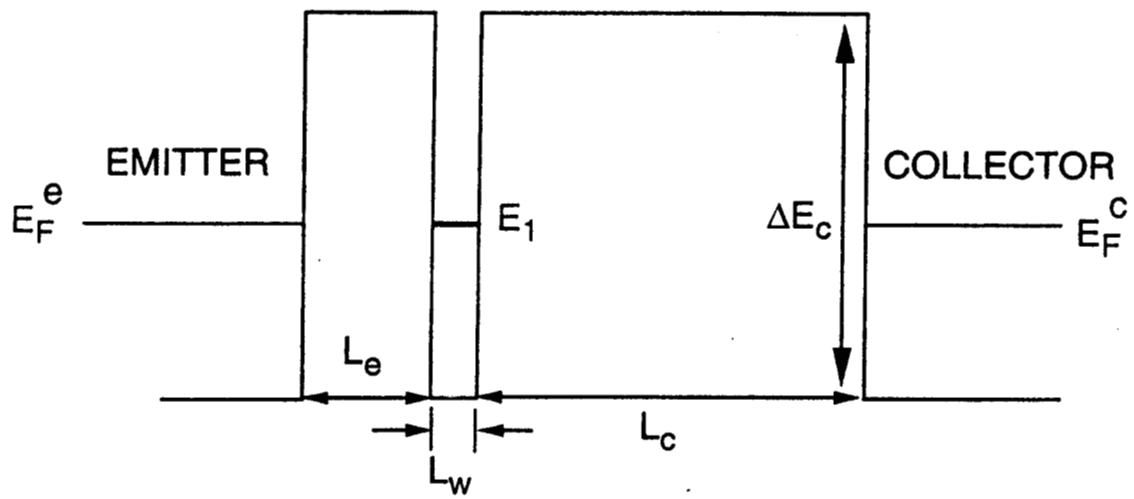
Fig 3: Experimental dark current and calculated dark current vs bias voltage at $T = 77\text{K}$. The theoretical model includes current contributions from resonance tunneling, non-resonance tunneling and thermionic emission as described in the Eq. (1) to (11). The mobility $\mu=2000\text{ cm}^2/\text{Vs}$ and saturated drift velocity $v_s=5\times 10^6\text{ cm/s}$ were obtained from the theoretical fit.

Fig. 4: Calculated resonance tunneling current contribution (described by Eqs. 6 and 7) to the total dark current at $T = 77\text{ K}$. Negative current below 200 mV indicates a change in the direction of the resonance current (i.e. from well to emitter contact).

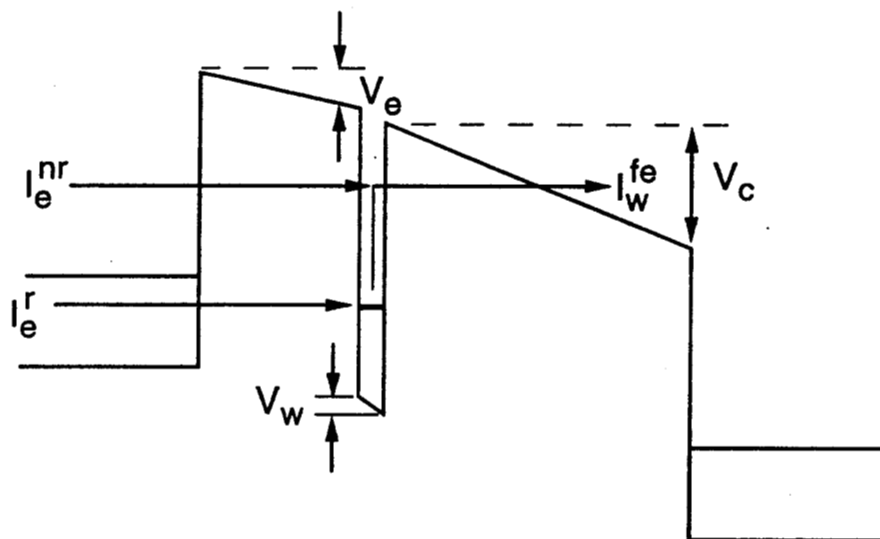
Fig. 5: Calculated potential drops across the emitter barrier (V_e), collector barrier (V_b) and the quantum well at $T = 77$ K as a function of total applied bias voltage.

Fig. 6: Calculated electron density in the quantum well at $T = 77$ K as a function of bias voltage. The drop in electron density at higher bias voltages is resulted from decrease in the resonant tunneling current. The photocurrent of the structure is expected to show similar behavior with a peak at 320 mV.

(a)



(b)



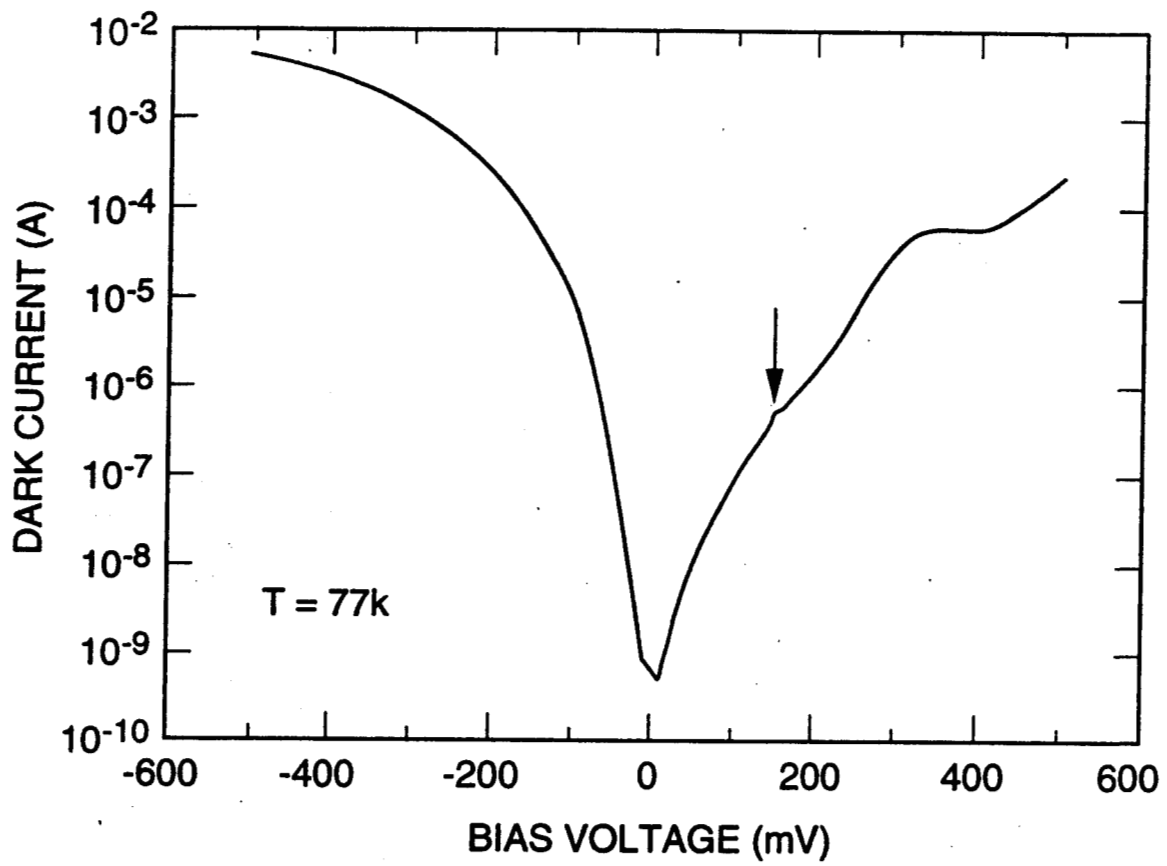


Fig 2 of 5

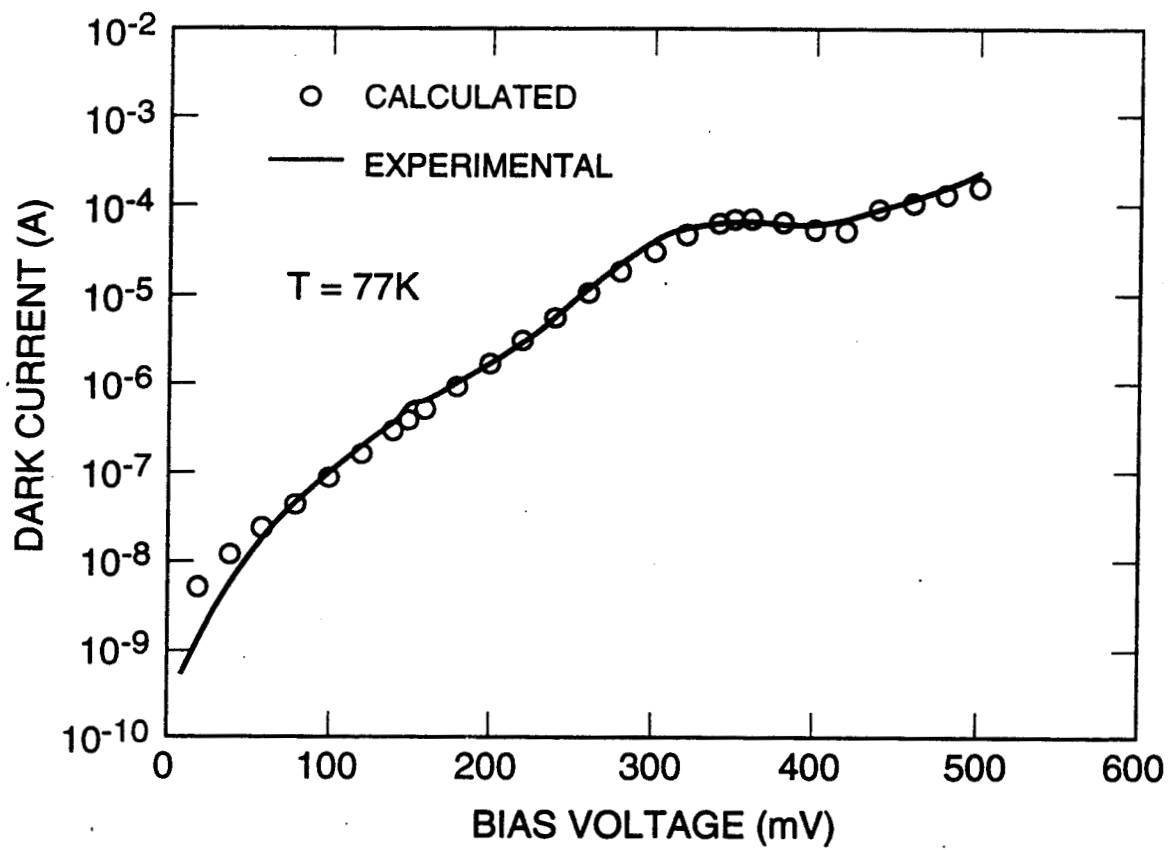


Fig 346

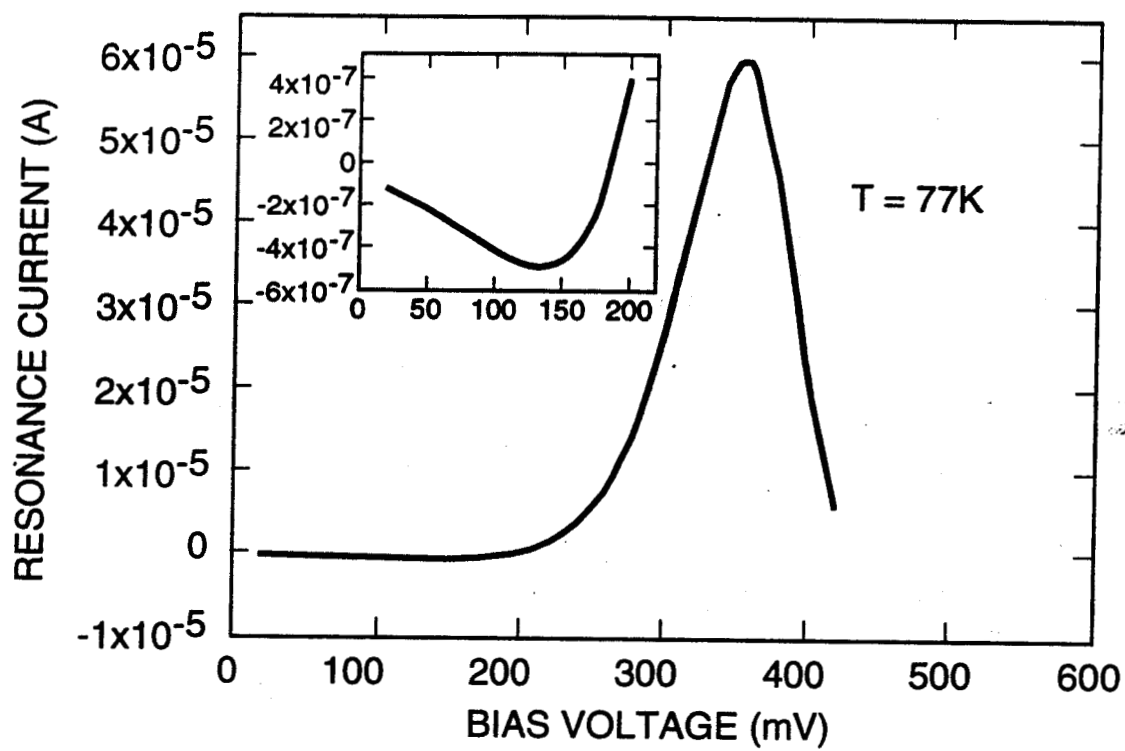


Fig 4 of 6

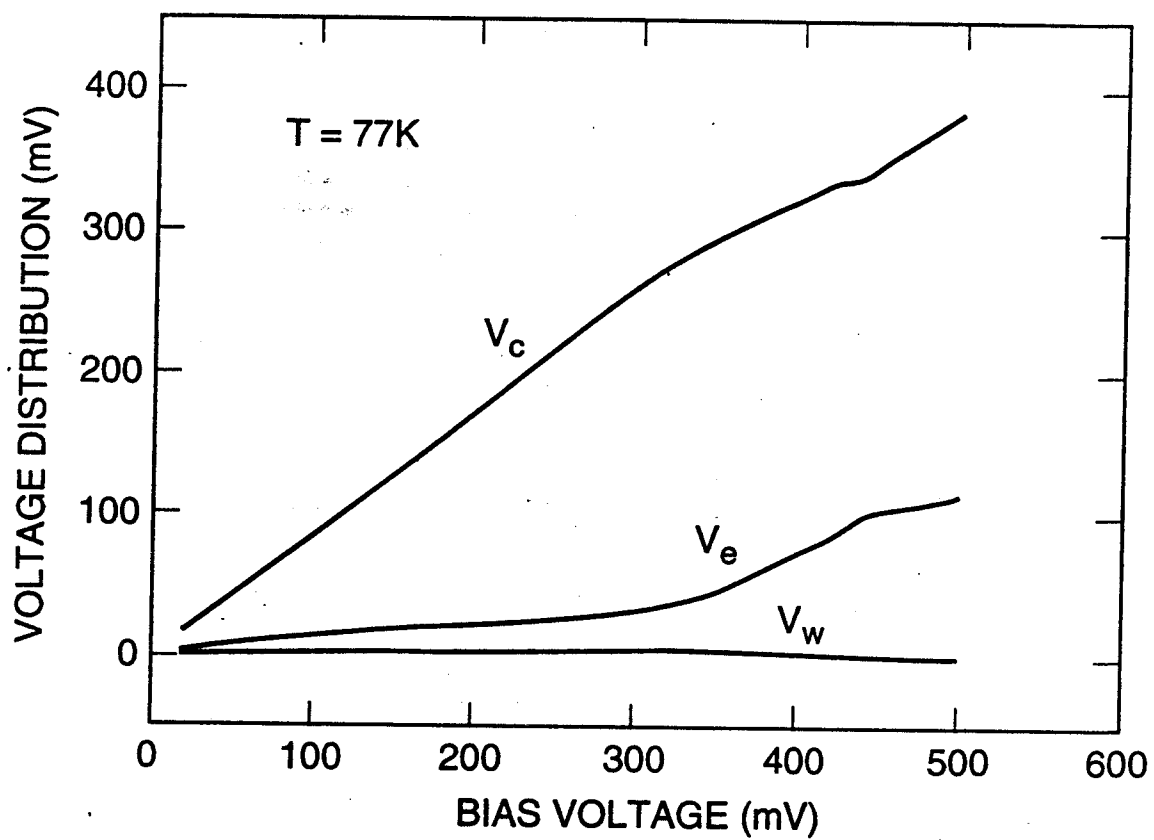


Fig 5 of 6

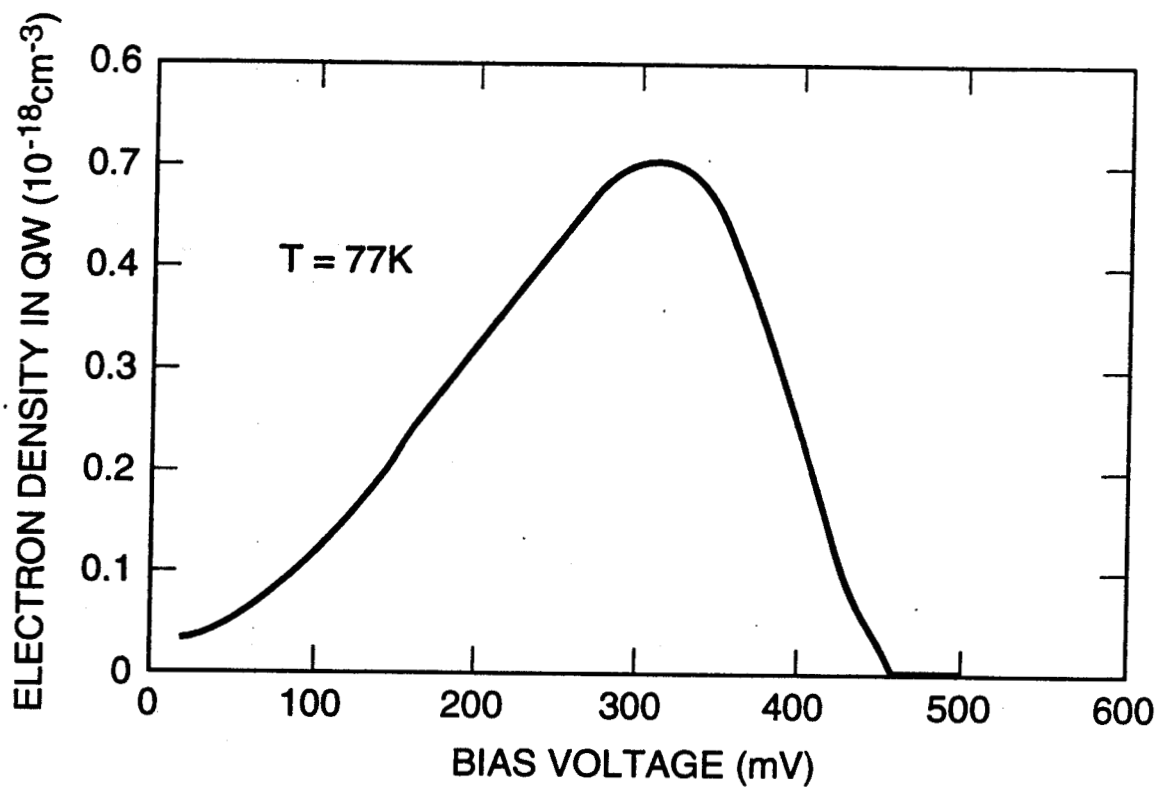


Fig 6.4.6